# Long-term trends and wave climate variability in the South Atlantic Ocean: the influence of climate indices

Natan Maia, Luis Pedro Almeida, João Luiz Nicolodi, Lauro Calliari, Bruno Castelle

# Long-term trends and wave climate variability in the South Atlantic Ocean: the influence of climate indices

Natan Z. Maia [a,b,*], Luis Pedro Almeida [c], João Luiz Nicolodi [a], Lauro Calliari [a], Bruno Castelle [b]

[a] *Universidade Federal do Rio Grande "FURG" - Instituto de Oceanografia - Laboratório de Oceanografia Geológica.* Av. Itália, CP 474, Rio Grande, RS, 96201-900, Brazil. natanzambroni@gmail.com; joaoluiznicolodi@gmail.com; calliarilauro@gmail.com

[b] *Univ. Bordeaux, CNRS, Bordeaux INP, EPOC, UMR 5805, F-33600 Pessac, France.* bruno.castelle@u-bordeaux.fr

[c] *CoLAB +Atlantic – Edifício Diogo Cão, Doca de Alcântara Norte, 1350-352. Lisboa, Portugal.* melolp@gmail.com

*Corresponding author: natanzambroni@gmail.com

*Universidade Federal do Rio Grande "FURG" - Instituto de Oceanografia - Laboratório de Oceanografia Geológica.* Av. Itália, CP 474, Rio Grande, RS, 96201-900, Brazil.

## ABSTRACT

Linking wave climate variability and trends with climate indices is important to better understand and predict large-scale patterns of wave variability down to wave conditions at the coast. This study investigates such links in the South Atlantic Ocean using 72 years of ERA5 wave hindcast. Different wave parameters are computed, including storm wave statistics, and are further analyzed in terms of long-term trends and interannual changes. Our results indicate that, over the last decades, wave height has been significantly increasing across the entire domain, while extreme events statistics are also increasing, although with more complex spatial variability. The variations of these wave properties are primarily correlated, from low to high latitudes, with the Atlantic Multidecadal Oscillation (AMO), Tropical Southern Atlantic Index (TSA) and Southern Annular Mode (SAM), with different preferred timescales. We think that better understanding and predicting the evolution of these climate indices, including under climate change, will be critical to anticipate coastal hazards in this region.

**Keywords:** South Atlantic Ocean; Wave climate; Storm waves; long-term trends; interannual variability; Climate indices.

## 1. Introduction

The generation and propagation of ocean waves is of great practical significance presenting far-reaching implications for coastal areas (Babanin et al., 2019; Reguero et al., 2019). The wave climate on the world's coasts is highly variable in both time and space. At the coast, ocean waves drive nearshore currents and sea water level variations through depth-induced breaking, with wave-driven processes control sediment transport as well as shoreline shape and changes (Castelle and Masselink, 2023). Extreme wave events can also cause coastal flooding and threaten coastal installations and protection structures (Van der Meer et al., 2016; Mentaschi et al., 2017). The wave climate therefore deeply affects where and how coastal and offshore infrastructures such as harbors and wave power generation plants can be built (Reguero et al., 2013, 2019). It is thus critical to understand the ocean wave climate variability and trends (Barnard et al., 2015; Mentaschi et al., 2017; Marshall et al., 2018; Reguero et al., 2019; De Leo et al., 2021; Maia et al., 2022). In addition, according to Morim et al. (2019), approximately 50% of the world's coastline is at risk from wave climate change, with ~40% revealing robust changes in wave properties.

Ocean surface gravity waves are generated by winds flowing across ocean basins and are thus intrinsically linked to atmospheric variability (Hemer et al., 2010; Reguero et al., 2012). It has long been known that atmospheric and oceanic circulation shows large-scale patterns of variability on interannual and longer timescales, which is reflected in wave climate variability (Garner et al., 2017; Castelle et al., 2017; Rasmussen et al., 2018; Vousdoukas et al., 2018; Oliveira et al., 2019). Large-scale patterns of atmospheric and/or oceanic variability are often addressed though climate indices such as the Southern Annular Mode (SAM) (also referred to as the high-latitude mode and the Antarctic Oscillation (AAO)), Tropical Southern Atlantic Index (TSA), Tropical Northern Atlantic Index (TNA), Western Hemisphere Warm Pool (WHWP) and the Atlantic Multidecadal Oscillation (AMO) (Thompson and Wallace 2000; Kerr 2000; Trenberth et al., 2002; Hemer et al., 2010; Reguero et al., 2013). Given that these patterns mostly superimpose and that waves are generated from different locations, the wave climate variability at a given location is modulated by the combination of several climate indices and teleconnections patterns (Castelle et al., 2017; Reguero et al., 2019; Silva et al., 2020; Maia et al., 2022), and a given

mode of variability can affect multiple ocean basins and hemispheres (Oliveira et al., 2019). According to Silva et al. (2020), in the recent decades the predominant wind-wave climate has been shifting in both direction and magnitude in both the Northern and Southern Hemispheres (Reguero et al., 2019), a phenomenon likely in response to altered atmospheric dynamics and interhemispheric teleconnections in association with increasing global temperature (Morim et al., 2019; Meucci et al., 2020; O'Grady et al., 2021).

The Southern Hemisphere (SH) has the most energetic ocean, Southern Ocean (Reguero et al., 2019), with waves generated by eastwards tracking, intense, extra-tropical cyclones impacting on almost all of the coasts globally (Hemer et al., 2010). According to Sterl and Caires (2005), 15% of the global wave variability is due to the swell propagating from the SH storm track region, and it governs the variability of the global mean. On SH, the Atlantic Ocean exhibits variability over a wide range of temporal and spatial scales but has pronounced variability at decadal and multidecadal timescales (Alexander et al., 2014). The SAM is the primary mode of variability in the atmospheric circulation of the SH extratropics and high latitudes (Marshall, 2003) and also, the primary mode influencing both wave height and directional variability beyond its energy flux both in medium and extreme conditions (Hemer et al., 2010; Mentaschi et al., 2017; Marshall et al., 2018).

There are some studies documenting the global warming trend associated with an increasing SAM trend over the past decades (Cai et al., 2003; Wang and Cai, 2013; Mentaschi et al., 2017), involving more frequent storms (Grassi et al., 2005) with potential implications for coastal sediment budgets and shoreline stability (Marshall et al., 2018). In addition to SAM, in the South Atlantic Ocean previous studies have also revealed strong relationships between changes in ocean–atmosphere interactions and the AMO index. According to Wang et al. (2008) and Kayano et al. (2019), the hurricanes and cyclones behaviors in the Atlantic Ocean are modulated by AMO oscillations, respectivly. Reguero et al. (2019) and Maia et al. (2022) identified strong correlations between the wave energy flux (*WEF*) and AMO behavior in the Southern Ocean and western South Atlantic Ocean, respectively. Another relevant climate index with important influence in the Atlantic Ocean is the TSA pattern which is associated with wave height increase in the northern equatorial Atlantic border of the continent and in

the Rio dela Plata area, whereas the *WEF* affects wave directionality (Reguero et al., 2013).

This paper investigates the wave climate variability (means and extreme events) and trend in the South Atlantic Ocean, and systematically addresses the links with the dominant regional modes of climate variability. This work is based on a 1950-2021 wave hindcast and a statistical analysis on wave and climate parameters. It will be shown that along the South Atlantic Ocean, wave climate variability is linked with, from low to high latitudes, AMO, TSA and SAM, together with increased duration, frequency and intensity of extreme events. Our results present new insights into the South Atlantic long-term wave climate variability and their drivers, including extreme conditions.

## 2. Data and Method

### *2.1 Wave hindcast*

In situ offshore wave data in the SH are scarce, with very few waverider buoy records compared to the NH. Global wave models thus provide a useful alternative to address the space and time variability and trends of wave conditions in the SH (Hemer et al., 2010). We used the 3-hourly 72-years global wave hindcast produced by the European Centre for Medium-Range Weather Forecasts (ECMWF) – ERA 5 (see Hersbach et al., 2020) from 1950 to 2021, from which significant wave height (*Hs*), peak wave period (*Tp*) and direction (*θ*) were extracted, from which the wave energy flux *WEF* was also computed (Antolínez et al., 2016; Mentaschi et al., 2017; Marshall et al., 2018; Reguero et al., 2019; Odériz et al., 2020a; Odériz et al., 2020b; Maia et al., 2022) through the equation:

$$WEF = \frac{\rho\, g^2\, Hs^2\, T}{64\,\pi} \qquad (1)$$

Where $\rho$ is the water density, $g$ the gravitational acceleration, $Hs$ significant wave height and $T$ the peak period. Outputs were extracted on a regular grid with 0.5° resolution covering the southern Atlantic Ocean between 5°N-60°S and 69.5°W-20°E, thus a total of 23,580 individual grid points. ERA5

validation for the South Atlantic Ocean is given in Odériz et al., 2020a, Odériz et al., 2020b, Maia et al., 2022 and Cotrim et al., 2022, with ERA5 showing a generally good performance in replicating wave high inter-annual variability compared to altimetry and buoy measurements. Three virtual wave buoys were used to address the spatial distribution of wave heights in deep waters along the South Atlantic Ocean: Nt: North; Ct: Central; St: South (Figure 1).

*2.2 Climate Indices*

Monthly teleconnection indices available since January 1950 were downloaded from the National Oceanic and Atmospheric Administration (NOAA) Physical Sciences Laboratory (www.psl.noaa.gov), nominally AMO (Enfield et al., 2001), WHWP (Wang et al., 2001), TSA (Einfield et al., 1999), TNA (Einfield et al., 1999). SAM (Marshall, 2003) was obtained from British Antarctic Survey (www.bas.ac.uk/), available since 1957.

*2.3 Analyzes*

2.3.1 Extreme events definitions

The peak over threshold method was applied on *Hs* to address extreme events (Dorsch et al., 2008). Following the definition by Masselink et al. (2014) and subsequently used in other studies, for each grid point an extreme event was defined as an event where *Hs* exceeded the 0.95 quantile (*Hs95*). A single extreme event was defined as a continuous period of *Hs* exceeding this threshold over at least 12 hours (Sénéchal et al., 2015; Angnuureng et al., 2017). Additionally, the individualization of extreme events was made through an independence criterion defined as when 30 hours elapsed between consecutive *Hs* records based on Almeida et al. (2011).

2.3.2 Extreme events statistics

We defined three parameters to study the extreme events behavior: duration (*D)*, frequency (F) and intensity (*I)*. For the duration, each year we calculated the number of hours under extreme conditions. The number of extreme events for each year was used to compute the storm frequency. Intensity (Karunarathna et al., 2014; Sénéchal et al., 2015; Angnuureng et al., 2017) was computed following Mendoza et al. (2011) through the following equation:

$$I = \int_{t1}^{t2} Hs(t)^2 dt \qquad (2)$$

where the extreme event duration starting and ending at *t1* and *t2*, respectively.

2.3.3 Correlation and trends

The yearly time series of all wave parameters described above were used to address the variability and trends of the wave climate. At each grid point, each climate index was used to compute correlations with the wave parameters, which were also linearly regressed to compute long-term trends. The statistical significance of correlations and trends for all variables was checked through a Student's t-test at a 95% level.

## 3. Results

### *3.1 Annual averages and trends of wave and extreme events*

Figure 2 shows the time-average (a-d) and long-term trend (e-h) of *Hs* and extreme events parameters for the entire South Atlantic Ocean between 1950 and 2021. The average *Hs* (Figure 2a) shows values between 0.5 and 4 m, with lower values close to coastal regions and gradually increasing towards higher latitudes to the south, especially to the southeast from latitude 36°S and to the southwest from latitude 55°S. The largest waves (*Hs* between 2.5 and 4 m) are predominantly incident from west quadrant. In contrast, the intertropical region shows smaller *Hs* between 0.5 and 1.5 m with a dominant southeast to northeast incidence as latitude decreases. The spatial distributions of time-averaged extreme event parameters show similar patterns, as the highest values of Intensity, Duration and Frequency of extreme events are observed in the temperate zone between latitudes 24 and 48°S, and below 48°S north of the Antarctic Peninsula and south of the African continent. For these regions, the highest values of cumulative Intensity are of the order of $1.5 \times 10^4$ $m^2$hr/year (Figure 2b), followed by an average accumulation of 250 hours of Duration in extreme conditions per year (Figure 2c) with records of up to 13 annual extreme events (Figure 2d). Figures 2b-d also reveals a localized area of large extreme event parameters with up to 16 events per year, for a total average yearly duration

of up to 800 hours and up to $0.7x10^4$ $m^2hr$ in Intensity in the region near the north coast of Brazil, in the Equatorial Atlantic.

The right-hand panels of Figure 2 highlight that all the wave parameters show an increasing trend, with areas where trends are not statistically significant essentially limited to a few points close to coordinates 5°N-36°W. Overall, the entire South Atlantic Ocean shows increasing yearly-average *Hs* (Figure 2e), at rates increasing southwards. The largest increasing *Hs* rates are located in the northern part of the Southern Ocean, ranging 1-1.2 cm/year. Intensity trends are mostly similar in patterns to that of *Hs*, peaking at 350 $m^2hr$/year between the American continent and Antarctica. In contrast, both Duration and Frequency trends show the highest increasing rates in the subtropical and tropical zones, with the exception of the northwest equatorial region. In addition to these areas, large Duration and Frequency increasing rates are observed in the southwestern region of the Atlantic Ocean, north of the Southern Ocean, up to 10 hours/year and 0.25 extreme events per year.

*3.2 Correlation with climate indices*

Table 1 shows the correlation between the main climate indices that influence the South Atlantic Ocean wave climate. TNA and WHWP indices show a high correlation with AMO (r = 0.82 and 0.7, respectively) and were thus discarded in the analysis below. In contrast, AMO, SAM and TSA systematically show low correlation between each other (r < 0.5) and are therefore assumed to result in contrasting correlation map with the computed wave parameters and are thus all kept for analysis.

**Table 1**. Correlation coefficients (r) between climate indices

| | **AMO** | **SAM** | **TNA** | **TSA** | **WHWP** |
|---|---|---|---|---|---|
| **AMO** | 1 | 0.46 | 0.82 | 0.26 | 0.7 |
| **SAM** | 0.46 | 1 | 0.36 | 0.39 | 0.47 |
| **TNA** | 0.82 | 0.36 | 1 | 0.32 | 0.75 |
| **TSA** | 0.26 | 0.39 | 0.32 | 1 | 0.41 |
| **WHWP** | 0.7 | 0.47 | 0.75 | 0.41 | 1 |

The left-hand panels of Figure 3 show the spatial distribution of the correlations between *Hs* and AMO, TSA and SAM indices. Interestingly enough, all climate indices mostly show a positive correlation, although with contrasting patterns. The highest correlations with the AMO (SAM) index are found in northern (southern) part of the domain, while TSA is dominant between latitudes 12 and 50°S. The right-hand panels of Figure 3 show the corresponding time series of *Hs* and dominant climate at three representative virtual buoys located in the three areas described above (North Nt, Central Ct and South St). The *Hs* anomalies identified at the Nt point have r = 0.65 with AMO, while the Ct point has r = 0.61 with TSA and to the south, St and SAM present r = 0.65. Interestingly, AMO shows a strong correlation with a clear multi-decadal variability, while TSA and SAM show a positive trend with superimposed interannual variability, which is reflected in the *Hs* variability at the selected virtual buoys.

Figure 4 shows the spatial distribution of correlations between the climate indices and the extreme events parameters, which, overall, are similar in patterns with those computed for *Hs*. At the Nt, Ct and St points, the indices that best correlate with variations in *Hs*, Duration, Frequency and Intensity are respectively AMO, TSA and SAM (Table 2).

**Table 2.** Correlation coefficients r between climate indices, *Hs* and extreme event parameters at North (Nt), Central (Ct) and South (St) points. The values in parentheses indicate the percentage of parameter variance explained by the climate index.

| | **Hs** | | | **Duration** | | | **Frequency** | | | **Intensity** | | |
|---|---|---|---|---|---|---|---|---|---|---|---|---|
| | **Nt** | **Ct** | **St** | **Nt** | **Ct** | **St** | **Nt** | **Ct** | **St** | **Nt** | **Ct** | **St** |
| **AMO** | 0.65 (42%) | 0.27 (7%) | 0.31 (10%) | 0.60 (36%) | 0.20 (4%) | 0.30 (10%) | 0.64 (41%) | 0.19 (4%) | 0.30 (9%) | 0.59 (35%) | 0.21 (4%) | 0.30 (9%) |
| **TSA** | 0.15 (2%) | 0.61 (37%) | 0.64 (41%) | 0.13 (2%) | 0.55 (30%) | 0.52 (27%) | 0.14 (2%) | 0.52 (27%) | 0.53 (28%) | 0.14 (2%) | 0.55 (30%) | 0.50 (25%) |
| **SAM** | 0.44 (19%) | 0.49 (24%) | 0.65 (42%) | 0.27 (7%) | 0.43 (19%) | 0.57 (33%) | 0.32 (10%) | 0.34 (12%) | 0.54 (29%) | 0.26 (7%) | 0.46 (21%) | 0.58 (34%) |

In order to provide insight into the wave field anomaly during the positive and negative phases of the dominant climate indices, Figure 5 shows the *Hs* and

*WEF* fields averaged over the 5 years with the strongest/positive and weakest/negative records of each climate index. The systematically positive (negative) anomaly observed for positive (negative) phases is in line with the positive correlations found in Figure 3. A notable exception is the positive anomaly in the northwest and southeast South Atlantic during the positive phase of TSA (Figure 5e). *WEF* anomalies provides new insight into the origin of the largest or smallest wave conditions during the positive and negative phases. In particular, during the positive phases of AMO and SAM, the large *Hs* positive anomaly at the largest latitude is clearly due to intensified wave energy flux travelling eastwards.

## 4. Discussion

From 1950 to 2021, overall the entire South Atlantic Ocean shows trends of waves and extreme events parameters increasing yearly-average. The positive *Hs* trend is in line with previous studies (Young et al., 2011; Reguero et al., 2013; Reguero et al., 2019; Oliveira et al., 2019; Odériz et al., 2020b; Maia et al., 2022; Cotrim et al., 2022). The largest increasing rates of *Hs* are located at higher latitudes, which is in line with Young et al. (2011) and Reguero et al. (2019). This increasing trend is largely explained by the greater occurrence of extreme conditions which is reflected in the increasing trend in Intensity. According to Young et al. (2011) and Reguero et al. (2019), at these high latitudes the Atlantic Ocean has some of the most extreme wave heights on the planet, and the Southern Ocean is the most energetic basin and dominates the other oceans in values and increasing rates of *WEF*.

Reguero et al. (2019) suggest that long-term changes in wave behavior need to be studied considering ocean atmosphere teleconnections and interannual variability. Although all climate indices have significant correlation values in virtually all points of the South Atlantic Ocean (Figure 3) there are areas of greater correlation for each index. The variations of *Hs* and extreme events parameters at the Nt point present higher correlation values with the AMO index (Table 2), which explains more than 42% of *Hs* variability, whereas the variability explanation of the extreme events parameters is between 35-41% (Table 2). As for the point Ct the TSA index explains 37% of *Hs* variance and that of the other parameters between 27-30%. Finally, the St point shows the largest correlation

with the SAM index for all parameters, explaining 42% of *Hs* variance and between 29-34% of the extremes. Climate indices are also strongly linked with the magnitude and direction of the *WEF* (Figure 5).

Figure 3d shows the co-variation between *Hs* at the Nt point and AMO phase alternation, especially on a multidecadal scale. The relationship between AMO and wave behavior in the Atlantic Ocean is in line with previous studies (Wang et al., 2008; Kayano et al., 2019; Reguero et al., 2019; Maia et al., 2022), showing that the positive and negative phases of AMO have a great influence on cyclone activities and on the *WEF* in the South Atlantic Ocean, especially on long-term time scales. Our findings (Fig. 5d) corroborate Reguero et al. (2019) who identified significant positive correlations between wave behavior and AMO on the coasts of Africa and Brazil. Maia et al. (2022) also suggested that the identified positive trends in the *WEF* are related to the transition of negative to positive AMO phase. During this transition phase, since the late 1980s, Atlantic tropical cyclone activity has been shown to have largely increased in frequency and intensity (e.g., Elsner et al., 2000; Goldenberg et al., 2001; Emanuel, 2005; Webster et al., 2005). Reinforcing this, according to Wang et al. (2008) and Kayano et al. (2019) the low-level cyclones multidecadal variability in the South Atlantic are modulated by the AMO, and are more energetic during the positive phases. Thus, AMO patterns play an important role in the cyclone trajectories and consequently in the generation and propagation of waves along the South Atlantic.

For the Ct point, the highest correlations associated with the TSA index are also shown by Reguero et al. (2013), where the TSA pattern is associated with increase in the wave height and change in the *WEF* on the eastern edge of the American continent, especially in tropical and subtropical regions. According to the authors, this is mainly caused by Atlantic warming and the reinforcement of the south–east trade winds and the easterly winds in the western equatorial Atlantic because of a northward migration of the intertropical convergence zone.

In general, the highest positive correlation with wave climate in mid- to high-latitudes and in the Southern Ocean have been associated with SAM (Meehl et al., 2007; Hemer et al., 2010; Reguero et al., 2013; Wang and Cai 2013; Mentaschi et al., 2017; Marshall et al., 2018; Oliveira et al., 2019; Silva et al., 2020). The positive trend observed in SAM in recent decades (Figure 3f) is

consistent with earlier studies (Thompson and Wallace, 2000; Thompson and Solomon, 2002; Marshall, 2003; Cai et al., 2005; Cai and Cowan, 2007; Hemer et al., 2010; Marshall et al., 2018; Cotrim et al., 2022), showing that part of the trends obtained in *Hs* and in the extreme events parameters might be explained by an increase in the SAM index, evidenced by the relative contribution of the high-energy southerly swells in *WEF* (Figures 5c, f). Figures 2e-h indicate trends of significant increase in all analyzed properties in the region of point St and, according to Sterl and Caires (2005), the increasing *Hs* trend in the Southern Ocean is due to the increased number of storms in this region. Corroborating these results, Hemer et al. (2008), Reboita et al. (2009), Hemer et al. (2010), Maia et al. (2016) and Cotrim et al. (2022) suggest that the increased *Hs*, storminess and cyclogenetic activity near the South American coast are related to the positive SAM phases that intensifies the extratropical storm belt generating extreme winds related to extreme waves. As evidenced in Figure 3f, the SAM shows a strong correlation with an interannual *Hs* variability. According to Marshall et al. (2018) the SAM is a probable candidate for driving significant surface wave variations due to its large spatial scale (hemispheric) and temporal scale (up to season) and thus, may be a valuable source of wave variability predictability in the SH.

Long-term variations in SST anomalies coexist with oscillations in *Hs* and *WEF* which indicates the influence of temperature-driven atmospheric teleconnections on wave-generation cycles (Silva et al., 2020; Maia et al., 2022) and characterizing the climate indices as proxies for wave behavior (Mentaschi et al., 2017; Reguero et al., 2019). Especially, over the past several decades Antarctic ozone depletion and emissions of greenhouse gases have been forcing a positive trend of the SAM (Thompson and Wallace, 2000; Gillett and Thompson, 2003; Marshall, 2003; Hemer et al., 2010; Mentaschi et al., 2017). These scenarios can consequently be expected to result in continuing observed trends in the Southern Ocean wave climate including wave height increases, poleward shift of the storm tracks (Arblaster et al., 2011; Wang and Cai, 2013; Zheng et al., 2013) beyond considerable changes in the recurrence frequency of extreme events by the end of the 21st century, which are projected to occur twice as frequently along many areas, especially in the SH (Mentaschi eta al., 2017).

## 5. Conclusions

We investigated wave climate variations and trends in the South Atlantic Ocean between 1950 and 2021 and identified that *Hs* is increasing across this region. We also observed that the extreme events are stronger, longer and more frequent. The variation of these properties presents correlations with the AMO, TSA and SAM climate indices, mainly from low to high latitudes respectively. During the positive (negative) phases of each index, higher (lower) *Hs* and *WEF* are observed, as well as predominantly west (east) swell. We consider that, given these indices show strong correlation with wave climate variation and trends, they are critical to understanding and predicting coastal hazards such as flooding and erosion in the South Atlantic Ocean to support the development of coastal management plans. Better understanding the influence of climate change on these climate indices should also improve our understanding of the impact of climate change on coastal response in the future.


## Acknowledgments

The authors are grateful to “CAPES PRINT - Programa Institucional de Internacionalização” for the financial support. NZM is sponsored by CAPES (Finance Code 001).

## Funding

This research was funded by CAPES-PRINT, Brazil under contract number 88887.578354/2020-00.


## Declarations of competing interest

The authors declare that they have no known competing financial interests or personal relationships that could have appeared to influence the work reported in this paper.

## 6. References


Alexander, M. A., Kilbourne, K. H. & Nye, J. A., 2014. Climate variability during warm and cold phases of the Atlantic Multidecadal Oscillation (AMO) 1871-2008. Journal of Marine Systems, 133, 14-26, DOI: https://doi.org/10.1016/j.jmarsys.2013.07.017

Almeida, L. P., Ferreira, Ó., Vousdoukas, M. I., & Dodet, G., 2011. Historical variation and trends in storminess along the Portuguese South Coast. Natural Hazards and Earth System Science, 11(9), 2407–2417. https://doi.org/10.5194/nhess-11-2407-2011

Angnuureng, D. B., Almar, R., Senechal, N., Castelle, B., Addo, K. A., Marieu, V., & Ranasinghe, R., 2017. Shoreline resilience to individual storms and storm clusters on a meso-macrotidal barred beach. Geomorphology, 290(August 2015), 265–276. https://doi.org/10.1016/j.geomorph.2017.04.007

Antolínez, J. A. A., Mendez, F.J., Camus, P., Vitousek, S., González, E.M., Ruggiero, P. & Barnard, P., 2016. A multiscale climate emulator for long-term morphodynamics (MUSCLE- morpho), Journal of Geophysical. Research-Oceans, 121, 775–791, doi:10.1002/2015JC011107.

Arblaster, J. M., G. A. Meehl, and D. J. Karoly., 2011. Future climate change in the Southern Hemisphere: Competing effects of ozone and greenhouse gases, Geophys. Res. Lett.,38, L02701, doi:10.1029/2010GL045384.

Babanin, A. v., Rogers, W. E., de Camargo, R., Doble, M., Durrant, T., Filchuk, K., Ewans, K., Hemer, M., Janssen, T., Kelly-Gerreyn, B., Machutchon, K., McComb, P., Qiao, F., Schulz, E., Skvortsov, A., Thomson, J., Vichi, M., Violante-Carvalho, N., Wang, D., … Young, I. R., 2019. Waves and swells in high wind and extreme fetches, measurements in the Southern Ocean. Frontiers in Marine Science, 6(JUL), 1–12. https://doi.org/10.3389/fmars.2019.00361

Barnard, P. L. et al., 2015. Coastal vulnerability across the Pacific dominated by El Niño/Southern Oscillation. Nature Geosci.8, 801–807

British Antarctic Survey. www.bas.ac.uk/. Access in 06/13/2022

Cai, W. & Cowan, T., 2007. Trends in Southern Hemisphere Circulation in IPCC AR4Models over 1950–99: Ozone Depletion versus Greenhouse Forcing. J. Clim.20,681–693.

Cai, W., Shi, G., Cowan, T., Bi, D. & Ribbe, J., 2005. The response of the southern annular mode, the east Australian Current, and the southern midlatitude ocean circulation to global warming. Geophys. Res. Lett.32, L23706.

Cai WJ, Whetton PH, Karoly DJ., 2003. The response of the Antarctic Oscillation to increasing and stabilized CO2.Journal of Climate16:1525 – 1538

Castelle, B., Dodet, G., Masselink, G., & Scott, T., 2017. A new climate index controlling winter wave activity along the Atlantic coast of Europe: The West Europe Pressure Anomaly. Geophysical Research Letters, 44(3), 1384–1392. https://doi.org/10.1002/2016GL072379

Castelle, B., Masselink, G., 2023. Morphodynamics of wave-dominated beaches. Cambridge Prisms: Coastal Futures, 1, e1, 1–13, https://doi.org/10.1017/cft.2022.2

Cotrim, C.S.; Semedo, A.; Lemos, G. Brazil Wave Climate from a High-Resolution Wave Hindcast.Climate., 2022. 10, 53. https://doi.org/10.3390/cli10040053

De Leo, F., Besio, G., & Mentaschi, L., 2021. Trends and variability of ocean waves under RCP8.5 emission scenario in the Mediterranean Sea. Ocean Dynamics, 71(1), 97–117. https://doi.org/10.1007/s10236-020-01419-8

Dorsch, W., Newland, T., Tassone, D., Tymons, S., Walker, D., 2008. A statistical approach to modeling the temporal patterns of ocean storms. J. Coast. Res. 24 (6), 1430–1438

Elsner, J. B., T. Jagger, and X.-F. Liu., 2000. Changes in the rates of North Atlantic major hurricane activity during the 20th century, Geophys. Res. Lett.,27, 1743–1746, DOI:10.1029/2000GL011453

Emanuel, K., 2005. Increasing destructiveness of tropical cyclones over the past 30 years, Nature,436, 686–688, PubMed, doi:10.1038/nature03906

Enfield, D.B., A.M. Mestas, D.A. Mayer, and L. Cid-Serrano., 1999: How ubiquitous is the dipole relationship in tropical Atlantic sea surface temperatures? JGR-O, 104, 7841-7848

Enfield, D.B., A. M. Mestas-Nunez and P.J. Trimble., 2001: The Atlantic multidecadal oscillation and it's relation to rainfall and river flows in the continental U.S.. Geophysical Research Letters, Vol. 28, 2077-2080.

Garner, A. J., Mann, M. E., Emanuel, K. A., Kopp, R. E., Lin, N., Alley, R. B., Horton, B. P., DeConto, R. M., Donnelly, J. P., & Pollard, D., 2017. Impact of climate change on New York City's coastal flood hazard: Increasing flood heights from the preindustrial to 2300 CE. Proceedings of the National Academy of Sciences of the United States of America, 114(45), 11861–11866. https://doi.org/10.1073/pnas.1703568114

Gillett, N.P. & Thompson, D.W.J., 2003. Simulation of recent Southern Hemisphere climate change. Science302: 273 – 275.

Goldenberg, S. B., C. W. Landsea, A. M. Maestas-Nunez, and W. M. Gray., 2001. The recent increase in Atlantic hurricane activity: Causes and implications, Science,293, 474–479, PubMed, doi:10.1126/science.1060040.

Grassi, B., G. Redaelli, and G. Visconti., 2005. Simulation of Polar Antarctic trends: Influence of tropical SST,Geophys. Res. Lett.,32, L23806. Doi:10.1029/2005GL023804.

Hemer, M. A., Church, J. A., & Hunter, J. R., 2010. Variability and trends in the directional wave climate of the Southern Hemisphere. International Journal of Climatology, 30(4), 475–491. https://doi.org/10.1002/joc.1900

Hemer, M.A., Simmonds I, Keay K., 2008. A classification of wave generation characteristics during large wave events on the Southern Australian margin. Continental Shelf Research28: 634 – 652

Hersbach, H., Bell, B., Berrisford, P., Hirahara, S., Horányi, A., Muñoz-Sabater, J., Nicolas, J., Peubey, C., Radu, R., Schepers, D., Simmons, A., Soci, C., Abdalla, S., Abellan, X., Balsamo, G., Bechtold, P., Biavati, G., Bidlot, J., Bonavita, M., … Thépaut, J. N., 2020. The ERA5 global reanalysis. Quarterly Journal of the Royal Meteorological Society, 146(730), 1999–2049. https://doi.org/10.1002/qj.3803

Kayano, M. T., Rosa, M. B., Rao, V. B., Andreoli, R. V., & de Souza, R. A. F., 2019. Relations of the low-level extratropical cyclones in the southeast Pacific and South Atlantic to the Atlantic multidecadal oscillation. Journal of Climate, 32(14), 4167–4178. https://doi.org/10.1175/JCLI-D-18-0564.1

Karunarathna, H., Pender, D., Ranasinghe, R., Short, A.D., Reeve, D.E., 2014. The effects of storm clustering on beach profile variability. Mar. Geol. 348, 103–112

Kerr, R. A., 2000. A North Atlantic climate pacemaker for the centuries. *Science*, *288* (5473), 1984–1986. https://doi.org/10.1126/science.288.5473.1984

Maia, N. Z., Calliari, L. J. & Nicolodi, J. L., 2016. Analytical model of sea level elevation during a storm: Support for coastal flood risk assessment associated with cyclone passage. Continental Shelf Research, 124, 23–34. https://doi.org/10.1016/j.csr.2016.04.012

Maia, N. Z., Almeida, L. P., Emmendorfer, L., Nicolodi, J. L., & Calliari, L., 2022. Wave climate trends and breakpoints during the Atlantic Multidecadal

Oscillation (AMO) in southern Brazil. *Ocean and Coastal Research*, *2022*, 22027. https://doi.org/10.1590/2675-2824070.21086nzm

Marshall, G. J., 2003. Trends in the Southern Annular Mode from observations and reanalyses .J. Clim.16, 4134–4143.

Marshall, A. G., Hemer, M. A., Hendon, H. H. & Mcinnes, K. L., 2018. Southern annular mode impacts on global ocean surface waves. Ocean Modelling, 129, 58–74. https://doi.org/10.1016/j.ocemod.2018.07.007

Masselink, G., Austin, M., Scott, T., Poate, T., & Russell, P., 2014. Role of wave forcing, storms and NAO in outer bar dynamics on a high-energy, macro-tidal beach. Geomorphology, 226, 76–93. https://doi.org/10.1016/j.geomorph.2014.07.025

Meehl, G., Stocker, T., Collins, W., Fiedlingstein, P., Gaye, A., Gregory, Kitoh, A., Knutti, R.,Murphy, J., Noda, A., Rper, S., Watterson, I., Weaver, A., Zhao, Z., 2007. Climate change2007: the physical science basis. Contribution of Working Group I to the Fourth Assessment Report of the Intergovernmental Panel on Climate Change, Chapter Global Climate Projections. Cambridge University Press, Cambridge, United Kingdom and New York, NY, USA. ISBN: 978-0-521-88009-1

Mendoza, E.T., Jimenez, J.A., Mateo, J., 2011. A coastal storms intensity scale for the Catalan sea (NW Mediterranean). Nat. Hazards Earth Syst. Sci. 11, 2453–2462

Mentaschi, L., Vousdouskas, M. I., Voukuvalas, E., Dosio, A. & Feyen, L., 2017. Global changes of extreme coastal wave energy fluxes triggered by intensified teleconnection patterns. Geophysical Research Letters. 44, 2416–2426.

Meucci, A., Young, I. R., Hemer, M., Kirezci, E., & Ranasinghe, R., 2020. Projected 21st century changes in extreme wind-wave events. Science Advances, 6(24), 1–10. https://doi.org/10.1126/sciadv.aaz7295

Morim, J., Hemer, M., Wang, X. L., Cartwright, N., Trenham, C., Semedo, A., Young, I., Bricheno, L., Camus, P., Casas-Prat, M., Erikson, L., Mentaschi, L., Mori, N., Shimura, T., Timmermans, B., Aarnes, O., Breivik, Ø., Behrens, A., Dobrynin, M., Andutta, F., 2019. Robustness and uncertainties in global multivariate wind-wave climate projections. Nature Climate Change, 9(9), 711–718. https://doi.org/10.1038/s41558-019-0542-5

National Oceanic and Atmospheric Administration (NOAA) Physical Sciences Laboratory (www.psl.noaa.gov, Access in 06/06/2022)

Odériz, I., Silva, R., Mortlock, T. R. & Mendoza, E., 2020a. Climate drivers of directional wave power on the Mexican coast. Ocean Dynamics, 70(9), 1253–1265. https://doi.org/10.1007/s10236-020-01387-z

Odériz, I., Silva, R., Mortlock, T. R., & Mori, N., 2020b. El niño-southern oscillation impacts on global wave climate and potential coastal hazards. Journal of Geophysical Research: Oceans, 125, e2020JC016464. https://doi.org/10.1029/2020JC016464

O'Grady, J. G., Hemer, M. A., McInnes, K. L., Trenham, C. E., & Stephenson, A. G., 2021. Projected incremental changes to extreme wind-driven wave heights for the twenty-first century. Scientific Reports, 11(1), 1–8. https://doi.org/10.1038/s41598-021-87358-w

Oliveira, B. A., Sobral, F., Fetter, A., & Mendez, F. J., 2019. A high-resolution wave hindcast off Santa Catarina (Brazil) for identifying wave climate variability. Regional Studies in Marine Science, 32, 100834. https://doi.org/10.1016/j.rsma.201. Regional Studies in Marine Science, 32, 100834. https://doi.org/10.1016/j.rsma.2019.100834

Rasmussen, D. J., Bittermann, K., Buchanan, M. K., Kulp, S., Strauss, B. H., Kopp, R. E., & Oppenheimer, M., 2018. Extreme sea level implications of 1.5 °c, 2.0 °c, and 2.5 °c temperature stabilization targets in the 21st and 22nd centuries. Environmental Research Letters, 13(3). https://doi.org/10.1088/1748-9326/aaac87

Reboita, M. S., Ambrizzi, T. & Rocha, R. P., 2009. Relationship between the Southern Annular Mode and southern hemisphere atmospheric systems. Rev. Bras. Meteorol.24, 48–55.

Reguero, B. G., Losada, I. J. & Mendéz, F. J., 2019. A recent increase in global wave power as a consequence of oceanic warming. Nature Communications. 205, 1–14

Reguero, B. G., Méndez, F. J., & Losada, I. J., 2013. Variability of multivariate wave climate in Latin America and the Caribbean. Global and Planetary Change, 100, 70–84. https://doi.org/10.1016/j.gloplacha.2012.09.005

Reguero, B. G., Menéndez, M., Méndez, F. J., Mínguez, R., & Losada, I. J., 2012. A Global Ocean Wave (GOW) calibrated reanalysis from 1948 onwards.

Coastal Engineering, 65, 38–55. https://doi.org/10.1016/j.coastaleng.2012.03.003

Sénéchal, N., Coco, G., Castelle, B., & Marieu, V., 2015. Storm impact on the seasonal shoreline dynamics of a meso- to macrotidal open sandy beach (Biscarrosse, France). Geomorphology, 228, 448–461. https://doi.org/10.1016/j.geomorph.2014.09.025

Silva, A. P., Klein, A. H. F., Fetter-Filho, A. F. H., Hein, C. J., Méndez, F. J., Broggio, M. F., & Dalinghaus, C., 2020. Climate-induced variability in South Atlantic wave direction over the past three millennia. Scientific Reports, 10(1), 1–12. https://doi.org/10.1038/s41598-020-75265-5

Sterl A. & Caires S., 2005. Climatology, variability and extrema of ocean waves: the web-based KNMI/ERA-40 wave atlas. International Journal of Climatology25(7): 963 – 977

Thompson, D. W. J. & Wallace, J. M., 2000. Annular modes in the extratropical circulation. Part I: Month-to-month variability. J. Clim.13, 1000–1016.

Thompson, D. W. J. & Solomon, S., 2002. Interpretation of recent Southern Hemisphere climate change. Science296, 895–899.

Trenberth, K. E., J. M. Caron, D. P. Stepaniak, and S. Worley., 2002. Evolution of El Nin˜o Southern Oscillation and global atmospheric sur-face temperatures. J. Geophys. Res.,107(D8), 4065, doi:10.1029/2000JD000298

Van der Meer, J.W., Allsop, N.W.H., Bruce, T., De Rouck, J., Kortenhaus, A., Pullen, T., Schüttrumpf, H., Troch, P. and Zanuttigh, B., 2016. EurOtop, Manual on wave overtopping of sea defences and related structures. An overtopping manual largely based on European research, but for worldwide application www.overtopping-manual.com.

Vousdoukas, M. I., Mentaschi, L., Voukouvalas, E., Bianchi, A., Dottori, F., & Feyen, L., 2018. Climatic and socioeconomic controls of future coastal flood risk in Europe. Nature Climate Change, 8(9), 776–780. https://doi.org/10.1038/s41558-018-0260-4

Wang, G., & Cai, W., 2013. Climate-change impact on the 20th-century relationship between the Southern Annular Mode and global mean temperature. Scientific Reports, 3, 1–6. https://doi.org/10.1038/srep02039

Wang, C., and D.B. Enfield., 2001: The tropical Western Hemisphere warm pool, Geophys. Res. Lett., 28, 1635-1638.

Wang, C., Lee, S. K., & Enfield, D. B., 2008. Atlantic warm pool acting as a link between atlantic multidecadal oscillation and atlantic tropical cyclone activity. Geochemistry, Geophysics, Geosystems, 9(5). https://doi.org/10.1029/2007GC001809

Webster, P. J., G. J. Holland, J. A. Curry, and H.-R. Chang., 2005. Changes in tropical cyclone number, duration, and intensity in a warming environment. Science,309, 1844–1846 PubMed, doi:10.1126/science.1116448

Young, I. R., Zieger, S., and Babanin, A. V., 2011. Global trends in wind speed and wave height. Science332, 451–455. DOI: 10.1126/science.1197219

Zheng, F., J. Li, R. T. Clark, and H. C. Nnamchi., 2013. Simulation and projection of the Southern Hemisphere annular mode in CMIP5 models. J. Clim.,26(24), 9860–9879, doi:10.1175/JCLI-D-13-00204.1.

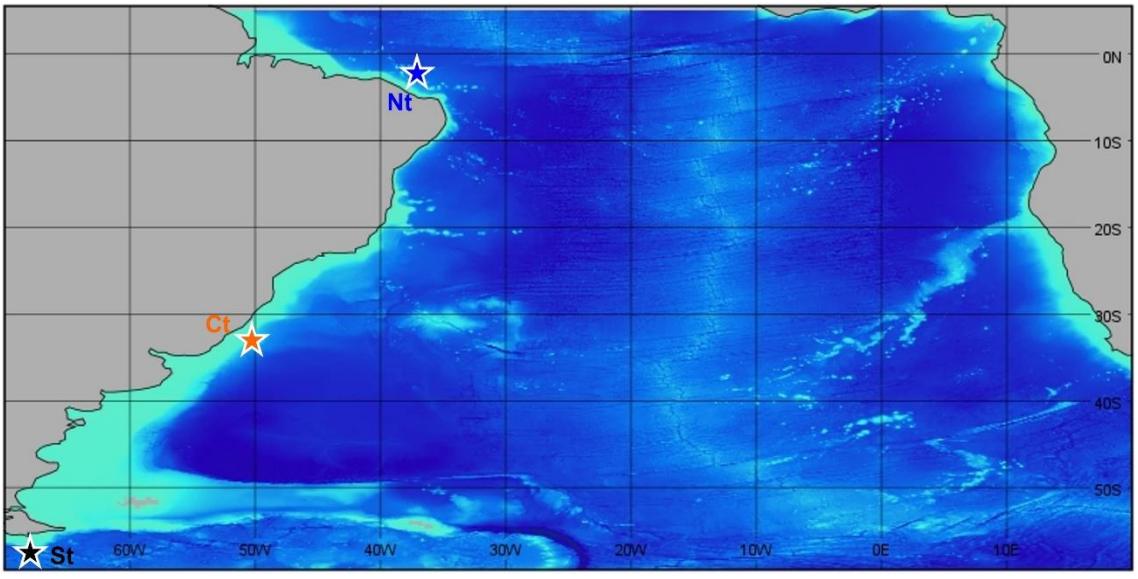


Fig. 1. Spatial domain for wave field. The locations of the North (Nt), Central (Ct) and South (St) virtual buoys are indicated by the colored stars. (For interpretation of the references to color in this figure legend, the reader is referred to the web version of this article.)

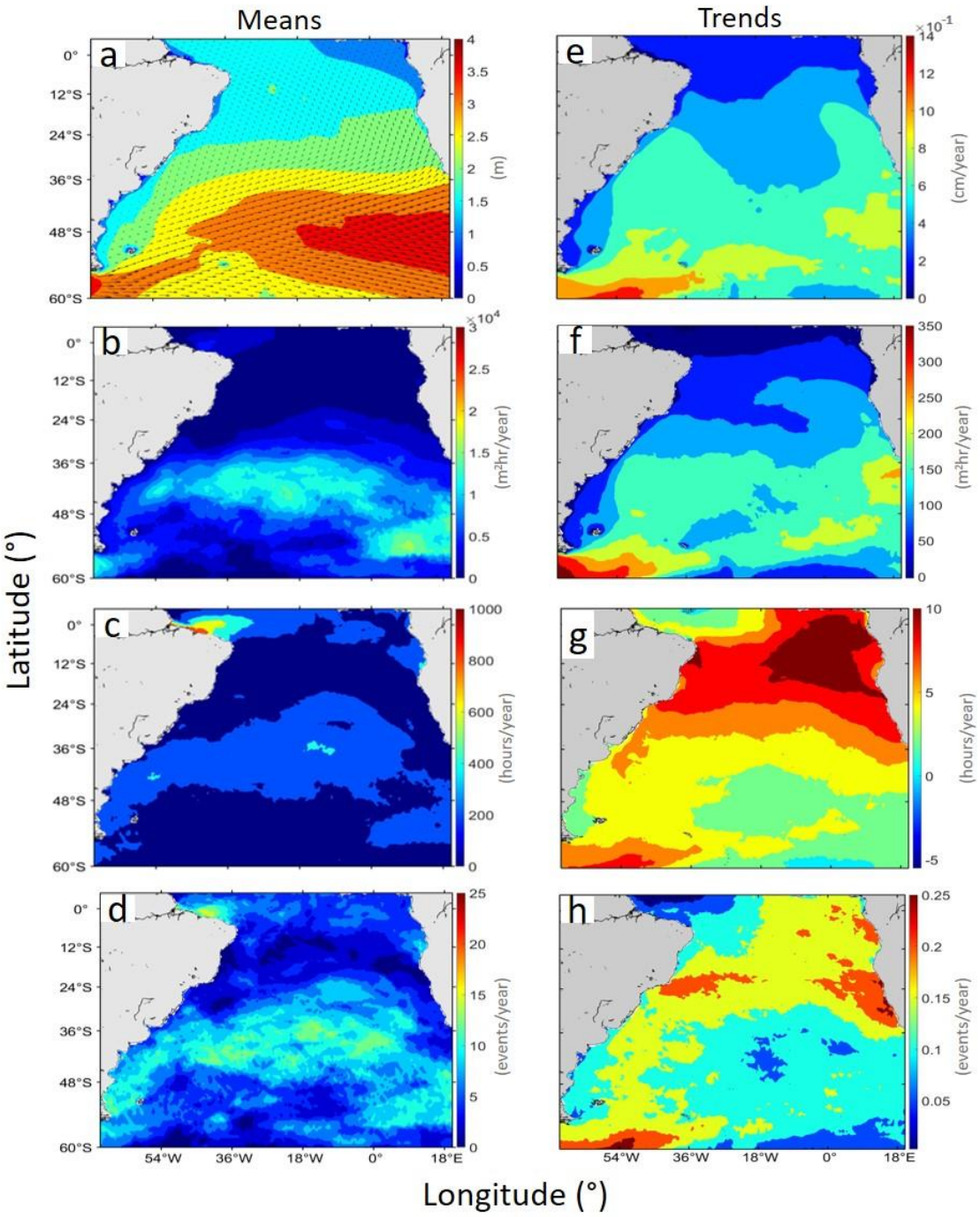


Fig. 2. Time average (left-hand panels) and increasing trend (right-hand panels) of Hs and extreme event parameters between 1950 and 2021: (a, e) Hs; (b, f) cumulative Intensity; (c, g) cumulative Duration; (d, h) Frequency. (a) it is the Hs average across the entire period and the arrows indication mean wave energy flux direction, while (b, c, d) are yearly average and (e, f, g, h) are the yearly increasing trends.

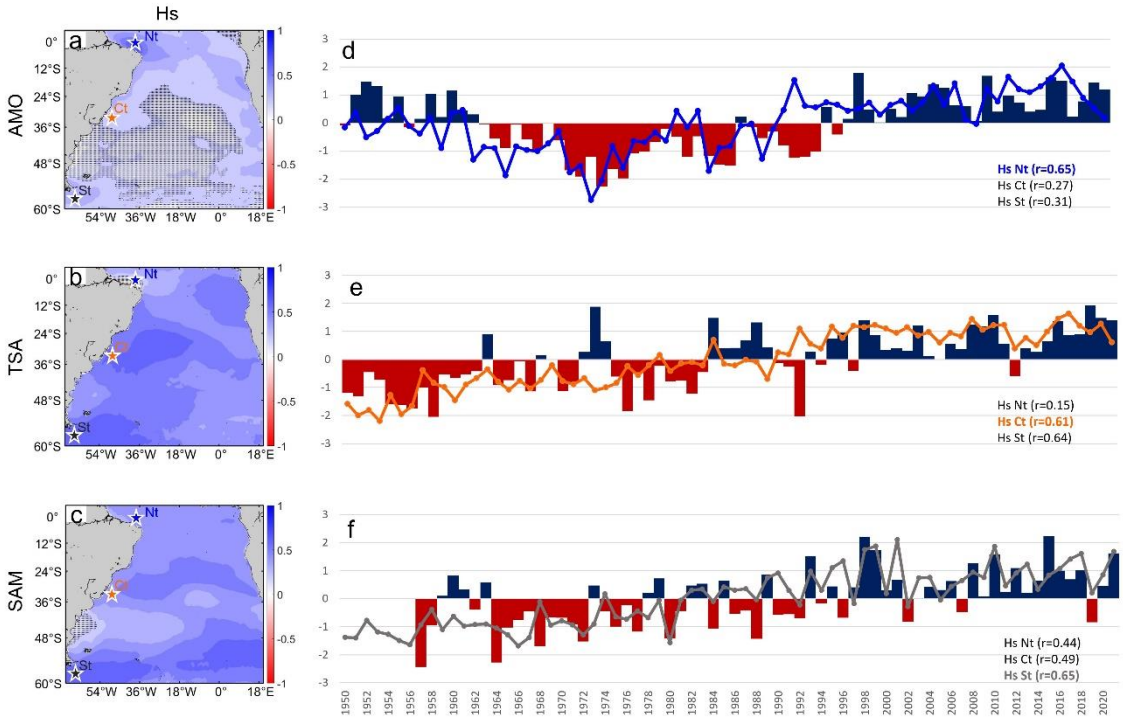


Fig. 3. Left-hand panels: spatial distribution of correlations between Hs and (a) AMO, (b) TSA and (c) SAM, respectively. The hatched areas show locations where correlation is not statistically significant. The locations of the North (Nt), Central (Ct) and South (St) virtual buoys are indicated by the colored stars. Right-hand panel: time series of Hs anomaly (solid lines) and the dominant climate index (colored bars) at the three virtual buoy locations, with computed correlations between Hs anomaly and the dominant index listed for all three virtual buoys: (d) Nt (dominant index: AMO) (e) Ct (TSA) (f) St (SAM)''. (For interpretation of the references to color in this figure legend, the reader is referred to the web version of this article.)

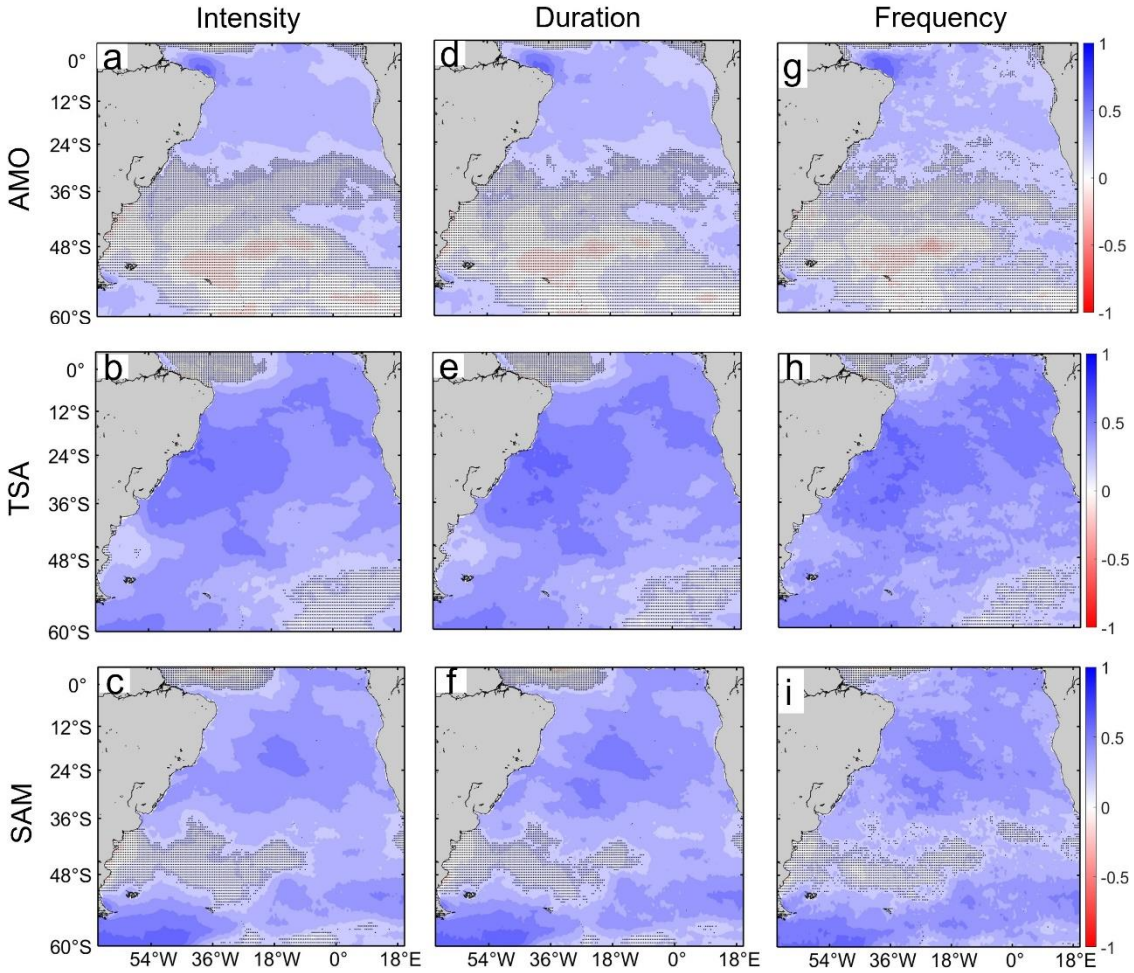


Fig. 4. Spatial distribution of correlations between extreme events parameters and climate indices considering the entire analyzed period. (a–c) Intensity; (d–f) Duration; (g–i) Frequency. The hatched areas show locations where correlation is not statistically significant.

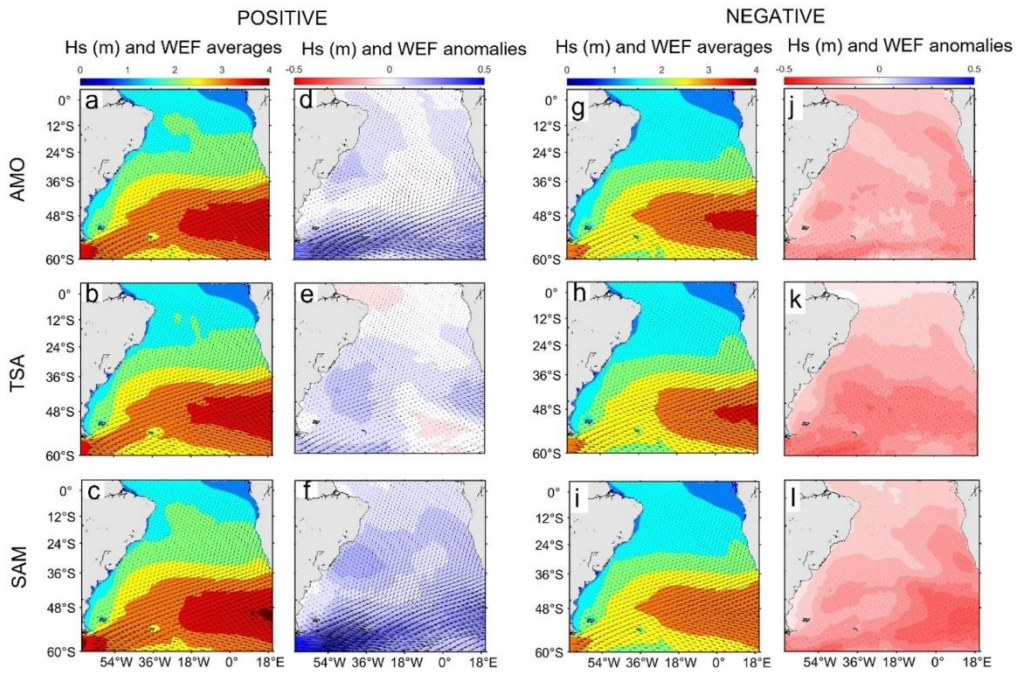


Fig. 5. Mean Hs and WEF and corresponding anomalies over the 5 years with the highest (left-hand panels, positive phase) and lowest (right-hand panels, negative phase) values of each climate index.